Available online at www.sciencedirect.com
ScienceDirect
C. R. Physique 9 (2008) 985–1001
COMPTES RENDUS PHYSIQUE
http://france.elsevier.com/direct/COMREN/

Recent advances in optical telecommunications / Avancées récentes en télécommunications optiques

New transmission systems enabling transparent network perspectives

A. Morea *, F. Leplingard, T. Zami, N. Brogard, C. Simonneau, B. Lavigne, L. Lorcy, D. Bayart

Alcatel-Lucent Bell Labs, centre de Villarceaux, France, route de Villejust, 91620 Nozay, France

Available online 28 November 2008

Abstract

The emergence of new devices and technologies introduces new trends and design issues for optical transport networks. The higher performance of transmission and switch systems enables the reduction of optoelectronic conversions in intermediate nodes with the introduction of transparency in the network. Simultaneously, the system of Automatic Switched Optical Networks (ASON) describes the rules for the construction of a network enabling cost reduction, above all for maintenance, and fast and automatic reconfiguration. Two axes have to evolve to make possible all these proprieties: the control plane and its relative set of protocols, to manage the network working for the network automation, and also the systems and tools enabling transparency and reconfigurability. In this article we focus on the second axis applied to an automatic transparent network. ***To cite this article: A. Morea et al., C. R. Physique 9 (2008).***

Résumé

Nouveaux systèmes de transmission permettant la conception des réseaux optiques transparents. L'apparition de nouveaux dispositifs et de nouvelles technologies permet d'envisager de façon nouvelle la conception des réseaux de transport optiques. L'amélioration des performances des systèmes de transmission et de commutation a permis de s'affranchir de conversions opto-électronique dans les nœuds intermédiaires et a ainsi rendu possible l'introduction de la transparence dans les réseaux. En parallèle, le concept de Réseaux Optiques à Commutation Automatique (Automatic Switched Optical Networks (ASON)) définit les règles de fonctionnement d'un réseau favorisant la réduction des coûts, principalement les coûts de maintenance, une plus grande disponibilité, ainsi qu'une reconfiguration plus rapide et automatique du réseau. Pour mettre en œuvre ces propriétés, deux axes de recherche sont envisagés : le plan de contrôle et ses différents protocoles dédiés à la gestion du réseau pour le rendre automatique comme les systèmes et les outils apportant transparence et reconfigurabilité. Dans cet article, nous analysons ce second axe appliqué à un réseau transparent automatique. ***Pour citer cet article : A. Morea et al., C. R. Physique 9 (2008).***

Keywords: Transparent optical network; Tunable, automatic and reconfigurable devices; Quality of transmission estimator; Planning and routing tools

Mots-clés : Réseau optique transparent ; Dispositifs accordables, automatiques et reconfigurables ; Estimateurs de la qualité de transmission ; Outils de planification et de routage

* Corresponding author.
E-mail address: annalisa.morea@alcatel-lucent.fr (A. Morea).

1631-0705/$ – see front matter
doi:10.1016/j.crhy.2008.10.018

1. Introduction

Recent technology evolutions have increased the reach of optical transmission, which, jointly with the introduction of optical cross-connects, avoid frequent optoelectronic (OEO) conversions. As a consequence, backbone optical networks tend to evolve from opaque (where OEO conversion is required systematically at each node) toward totally or partially transparent networks (where OEO conversions are, respectively, forbidden in intermediary nodes or made possible) [1]. In the following, totally transparent and partially transparent networks will be called transparent and hybrid, respectively.

Optical networks have been evolving also toward flexibility and automatic reconfiguration. ASON – Automatic Switched Optical Networks – [2] denotes these last two concepts of network suitable for both opaque and transparent/hybrid networks. The emergence and introduction of different devices and networking technologies have made this concept possible.

Fig. 1 illustrates the principal characteristics of future transparent network, the principal devices that make it possible (both already present in opaque networks and proper to transparent ones), and the interests behind these features. In the following we describe further how the identified devices make possible the features linked to an automatic transparent network. As we focus our attention only on systems we neglect all the protocol aspects associated to ASON; for more information, Ref. [3] addresses this subject in depth.

This article focuses on transparent core networks, which comprise the infrastructure interconnecting various smaller networks (metropolitan and/or local) through major locations, providing a path for the exchange of information between different sub-networks. Hereafter, we introduce the main devices linked to the emergence of transparent ASON:

1. *Wavelength switching technologies* (reconfigurable optical add-drop multiplexer – R-OADM – and wavelength selective switch – WSS) enable the automatic insertion/extraction of a channel at any wavelength and address any wavelength toward any direction in an optical way. Their presence avoids the need for human intervention to change the network configuration and so reduces the operational expenditure associated to the network management. Moreover, the possibility of a transparent node pass through allows transparent transmission and so enables the reduction of OEO devices, which induces a reduction of capital expenditure;
2. *Tunable devices*, such as transponders – TSP – and reconfigurable switches (R-OADM/WSS), work at different wavelengths and different loads. Their presence allows easy reconfiguration (wavelength coloring and output directioning) without resource over-dimensioning (capital and operational expenditure savings). The tunable compensators improve the transmission reach relative to a given bit-rate and modulation format making possible transparent transmission;
3. *Optical monitoring devices*: already present in opaque networks, they become essential if automatic reconfiguration of the network is envisaged. These devices supervise the network/path physical state and set off an alarm in

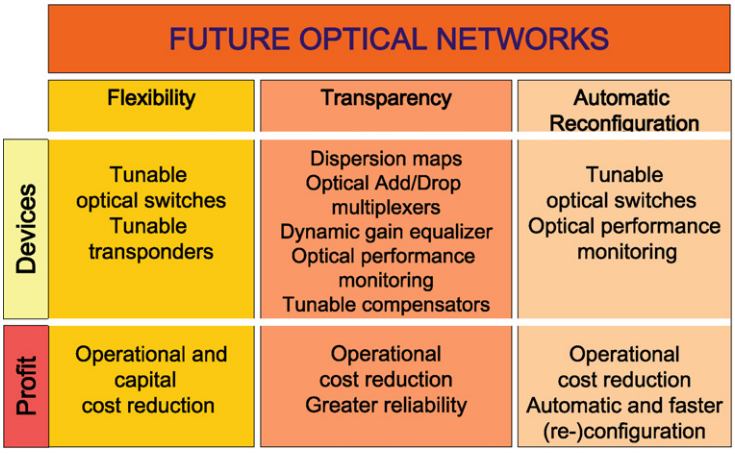

Fig. 1. Future transparent network characteristics and its interests.

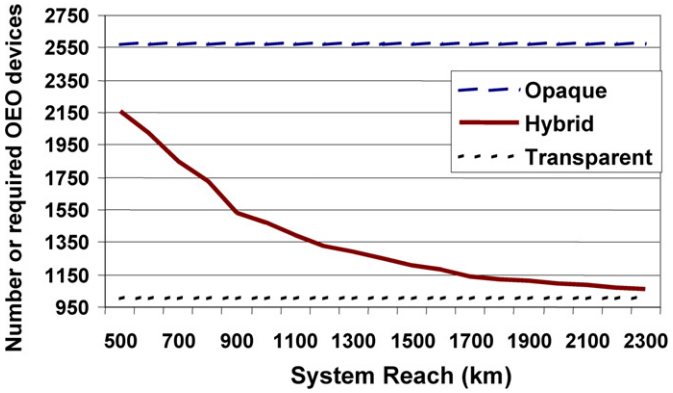

Fig. 2. Comparison of the number of optoelectronic devices required by opaque, transparent and hybrid networks for a European network composed by 39 nodes and 62 links with 500 demands.

case some physical degradation becomes too important and jeopardizes the feasibility of a transparent connection. Such devices are important for automatically reconfigurable networks in case of failures. Depending on the choice of the kind of monitoring and of the parameters to monitor, the performance/impairment monitoring can be more or less complicated [4];

4. *Dynamic equalizers and dispersion maps*: the transmission of a signal over very long distances is made possible thanks to dynamic gain equalization and dispersion maps, whose choice can increase the transmission reach [5].

The interests of transparent networks are numerous: greater flexibility to the introduction of new bit rates, transmission (SDH, ATM, [1]) and modulation formats, and scalability. Transponders are sensitive to all these characteristics; they have to be changed if one of them is modified.

The interest of WSS is their easy upgradeability with network size increase, in fact if the node connectivity (number of fibers connected to the node) grows up in an opaque network we need to insert multiplexers, eventually change the electrical node if the installed one does not have enough access ports (that has to be equal to the number of activated channels in the fibers). The number of activated channels depends on traffic evolution, as in transparent and hybrid networks OEO conversions are reduced. Therefore, there is easier adaptability to traffic evolutions and the over-dimensioning/changes of electrical cross-connects is minimized; similarly the number of additional OEO devices is reduced.

In a fully transparent network OEO devices are placed at the end points of the transmission, independently of the traversed nodes and links, while in opaque networks their number is proportional to the number of traversed nodes ($2 \times (N - 1)$). In hybrid networks their number is between values obtained for opaque and transparent networks and depends on system reach. Fig. 2 represents the number of required TSP for a European network, composed of 39 nodes and 62 links of average length 300 km (for more details about the network see [6]) and containing up to 80 wavelengths. 500 demands (extracted according to a uniform distribution of connection probability) are routed in the network. The number of total transponders (OEO devices required for insertion/extraction of demands and for optoelectronic regeneration) is computed for opaque (dashed lines) and transparent (dotted lines) networks, indicating the boundaries of the number of required OEO devices for a hybrid case as a function of the system reach. From Fig. 2 we can see that compared to opaque networks the introduction of transparency for a system reach of 500 km enables 16% reduction in the total number of OEO devices (used to insert/extract the traffic and for intermediate OEO conversion) and 60% reduction for a system reach of 2300 km.

The reduction in the number of optoelectronic devices also entails reducing the size of electronic switches and their price; moreover, fewer electronic devices and smaller routers reduce power consumption [7].

New technologies allow a greater exploitation of the fiber capacity by increasing the number of transported channels (dense wavelength division multiplexing – DWDM) making the network more flexible to evolution. The possibility to by-pass electronic switches makes the introduction of a huge number of channels in a fiber not cost restrictive, because electronic switches do not process the by-passed channels.

Table 1
Issues and features related to the opaque, transparent and hybrid networks.

	Opaque	Transparent	Hybrid
	OEO conversion at each node	No OEO conversion at intermediary node	Possible OEO conversion at intermediary node
Flexibility to bit rate	No	Partial	Partial
Flexibility to reconfiguration	Yes	Possible	Possible
OEO regeneration devices	Yes	No	Possible
OEO wavelength conversion devices	Yes	No	Possible
Physical impairment consideration in routing tools	No	Yes	Yes
Impairment compensation devices	Simple	Complex	Complex
Network upgradeability	Complex	Easy	Easy
Network extension	Unlimited	Limited	Unlimited
Network monitoring	Simple	Complex	Complex
Optimization of electronic resources	No	Yes	Yes
Availability performance	Highly dependent on electronic devices	Dependent on chosen route	In between transparent and opaque performance

The combination of tunable systems and automatic processes will make networks dynamic and autonomously flexible to better serve the changes of the traffic demands for emerging services. This also makes demand survivability, that is the reception of the optical signal even if one or more failures appear on the optical layer, less resource consuming [10]. In the near future it will be possible to change the network configuration without many human interventions, consequently reducing its operational cost. Moreover, transparent and hybrid networks perform on a higher level of availability as shown in [11].

The OEO conversion likelihood makes hybrid networks not sized limited because during the network planning it is possible to place OEO conversions where needed to avoid problems of wavelength continuity and physical feasibility.

Beyond these functional and economic features, transparency poses many technical challenges such as the consideration of physical impairments to evaluate the more appropriate route associated to a connection request. Routing tools are used to evaluate what path is best as a function of the number of devices and the quality of the signal at the reception.

Table 1 summarizes the main characteristics relative to opaque, transparent and hybrid networks.

Finally, we want to precise that transparency enables a reduction of the number of OEO devices, but additional and/or more sophisticated devices have to be introduced. Ref. [12] shows the possible capital expenditure (CAPEX) savings when transparency is introduced.

This paper is divided into three parts. Section 2 is devoted to the architecture of transparent/hybrid networks and we describe the principal devices and functions specific to the transparent network, in Section 3 the evolution of routing tools is described and finally in Section 4 the creation of the signal performance estimator is detailed. Global perspectives on future optical networks conclude this paper.

2. Architecture of a transparent network

A network is composed of nodes and links, as is depicted in Fig. 3. Link architecture remains the same as in the opaque case [12]. To ensure longer reaches the employed systems have improved performance, like for sub-marine transmission or terrestrial having ultra long links as in US. The elements and techniques needed for increase reach are: high performance amplifiers (low noise, flat gain), dynamic gain equalizers (DGE), FEC, polarization mode dispersion (PMD) compensation and new modulation formats. In a transparent network a chromatic dispersion management has to optimize the physical performance for the whole network and not for each specific link, as for the opaque case [5]. Dispersion management is ensured by the dispersion map, which is obtained by the succession of transmission fibers (with positive chromatic dispersion) and compensation fibers (with negative dispersion); the latter are also called dispersion chromatic modules (DCM). The fiber type usually used for transmission is the Single Standard Mode

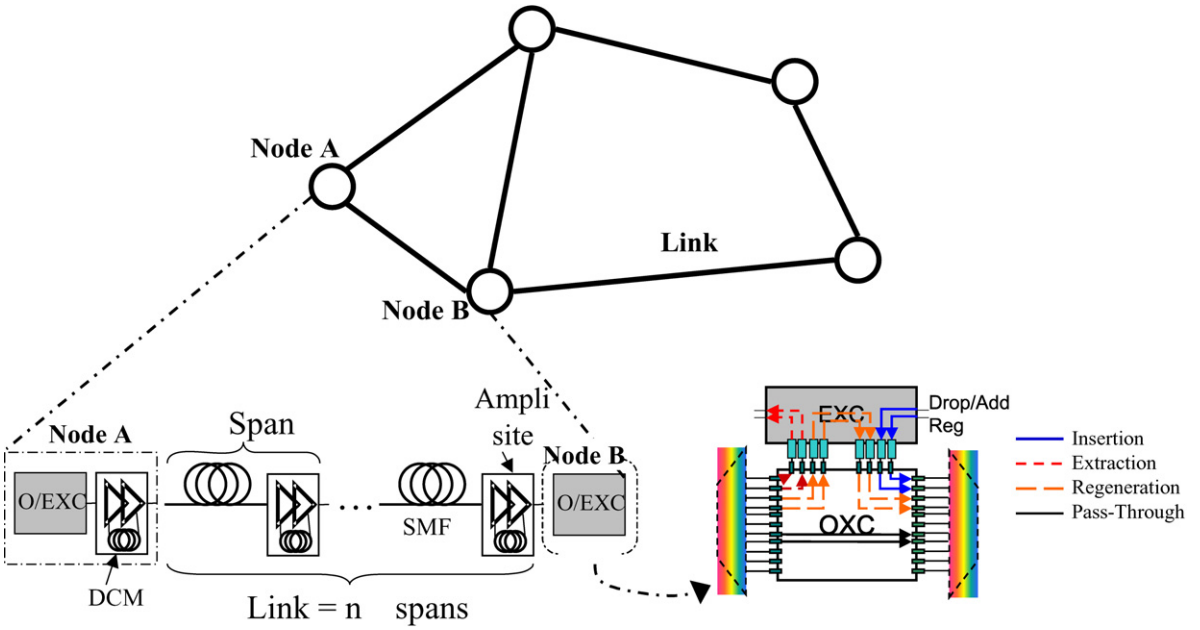

Fig. 3. Example of a transparent/hybrid optical network structure: its link and node architectures.

Fiber (SMF) [8] and for the compensation the Dispersion Compensating Fiber (DCF) [9]. In Fig. 3 the depicted link is composed of n spans, each one is made by a section of SMF followed by an amplification site ('Ampli site') containing a double amplifier within the DCM.

Nodes in transparent/hybrid networks have a completely different structure from the opaque case. In fact they have to present a fully optical stage (OXC) to switch channels, and also an electronic stage (EXC) to enable the insertion/extraction of signals (Add/Drop) and, in the case of hybrid networks intermediate, OEO conversions (Reg). Fig. 3 shows the subdivision of a node in these two stages and depicts how the signal traverses the different node stages.

Monitoring is required to allow reduced delay for the establishment of a connection and quality of service delivery. The monitored physical parameters are stored and these values are used to compute feasible path (see Section 3), without having the risk to do different path establishment because the physical performance is not considered before.

In this section we focus our attention on the optical switches and on the new monitoring functions.

2.1. Architecture for transparent optical cross-connect

Fig. 4 shows all the functions that are combined in a conventional WSS, a key element of a flexible optical network owing to its high integration level. In this picture there is an input fiber with m channels and the channels can be conveyed to any output fiber among the available N. When it is used as a reconfigurable optical de-multiplexer, the wavelength selective switch (WSS) [13] can steer each optical channel present on its input common port toward any of its output ports according to its wavelength by the means of an array of bi-axial Micro Electro Mechanical Systems (MEMS). One axis performs the beam steering toward one of the optical multiplexers connected to the output ports while the other rotation axis is used to slightly shift the optical ray and so to create a given attenuation level for the switched channel. If a signal traverses the WSS in the opposite direction, it then acts as a reconfigurable optical multiplexer; hence, the WSS-based node architectures as depicted in Fig. 5 (left side of the figure) allow the easy upgrade from a simple Reconfigurable Optical Add and Drop Multiplexer (R-OADM) to an Optical Cross-Connect (OXC) with the connectivity required by the operators [14]. In Fig. 5 we have a detailed representation of the optical stage for a node composed of WSS. At the state of the art there is no possible WSS with more than 10 output ports. $F_{\text{in/out}}$ depicts the input/output fibers respectively; λ-agile transmitters denote tunable OEO devices. On the right side of Fig. 5, the WDM comb of all the input ports is broadcasted toward all the output ports by the optical couplers. Then, at each output port, a WSS selects the channels that are transmitted to this port. This figure also illustrates that

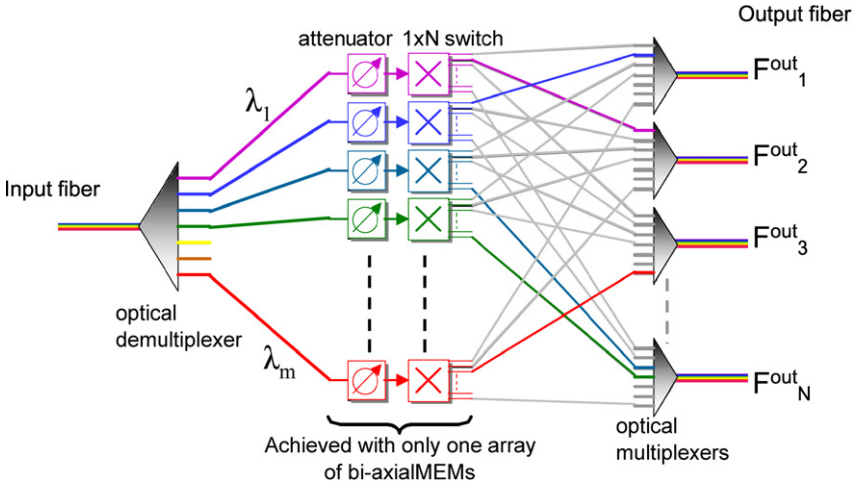

Fig. 4. Schematic diagram of a wavelength selective switch (WSS).

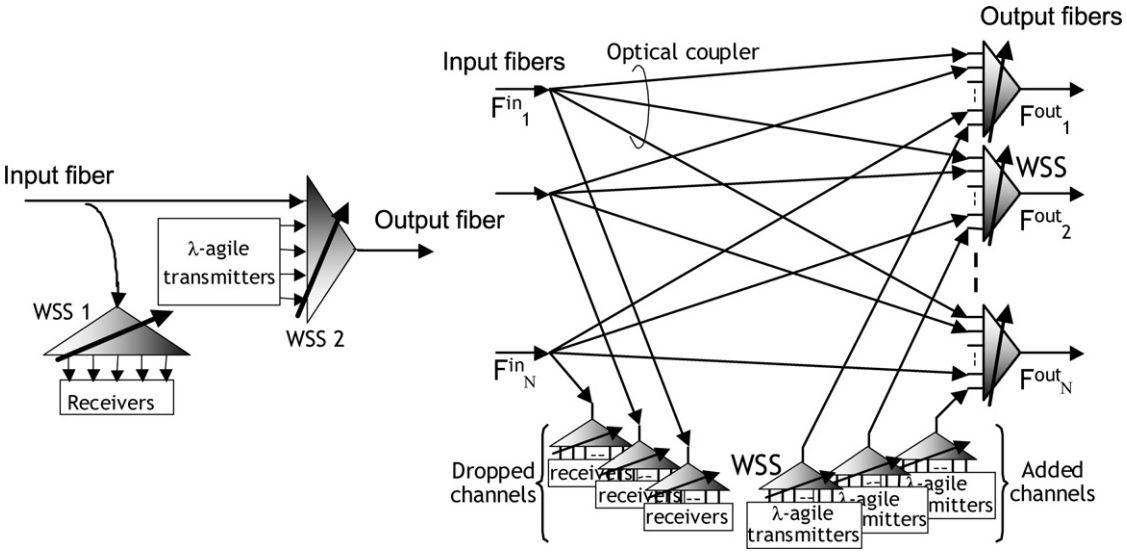

Fig. 5. Schematic diagram of a WSS-based ROADM (left) and a N-degree WSS-based OXC (right).

WSSs can also ensure the flexible insertion and extraction of channels (respectively “Add” and “Drop”). To ensure more flexibility such as the possibility for a channel to change not only the wavelength but also the output fiber, more complex node architecture are adopted. Such architecture enables channel restoration (see Section 3) that is very important to have fully flexible nodes.

2.2. In-line monitoring function and node devices

To make the network more automated, monitoring the physical features of the network is required. Complete information about the link physical state allows automatic systems to control how the network physical state evolves and if necessary to anticipate strong signal degradations that could produce reception errors by creating alternative paths. Ref. [15] gives us an example of how in an automatic and dynamic network the Polarization Mode Dispersion (PMD) monitoring can prevent PMD outages. The PMD outage is the loss of signal due to the high degradations caused by PMD. Monitoring consists in taking a small part of the optical signal by means of a tap coupler in order to detect the presence of optical power or to measure the physical features of the signal or transmission link. The monitoring has three main objectives:

1) To provide a complete knowledge of the network features to support the process of transmission quality estimation;
2) To enable the effective control of the optical tunable devices in the network that should compensate for physical degradations; and
3) To make the detection and localization of malfunctions quick and more precise.

The first objective is partial because it only addresses the physical parameters that could be inferred with a meaningful accuracy even if the investigated channel is not yet lighted up, as the Quality of Transmission (QoT) estimation is carried out before channel establishment (see Section 4). A solution to this issue could be the use of a probe signal to evaluate physical impairments that alter the transmission.

The second objective is very ambitious since the corresponding monitoring should be able to get relevant measurements on an operating network. Moreover, to reduce the associated cost, the monitoring devices should be shared between several fibers. It is the reason why the measurements should be fast, accurate and should not impact the transported traffic. The monitoring of the channel power at the nodes is already a standard functionality of the transparent network particularly to drive the channel attenuation in the network nodes. However, this functionality has still to be made truly independent of the power of the other channels and of the channel spectral power density. Ref. [17] shows how the power monitoring is affected by the presence of neighbor channels. The next issue is about Optical Signal to Noise Ratio (OSNR), PMD and chromatic dispersion monitoring; these measurements should not disturb controlled signals and should be obtained independently of the signal state. Notably, their accuracy should remain unchanged whatever amount of non-linearities or number of filters the signal undergoes.

The third monitoring objective is more conventional and is already present in current networks to quickly detect cable cuts. Because of the further implemented transparency, this monitoring should be more elaborated to detect and analyze the degradations that are indirect consequences of a failure in the network. If the evolution speed of the malfunction source is relatively slow, the monitoring can trigger a pro-active restoration process or fixing process [15]. It is also noticeable that this category of monitoring comprises controlling that correct channels are routed toward the correct output ports inside the optical cross-connects.

Detecting the principal impairments to be measured and how to integrate their real-time optical monitoring into the control plane is the scope of several studies, such as [16].

3. Planning tools

Dimensioning algorithms are the basic network design tools. Their goal is to evaluate the number of resources enabling the routing of all foreseen traffic requests and minimizing the total network cost at the same time. Strictly related to the dimensioning are the routing algorithms, i.e. the process of selecting paths in a network along which to send the traffic from a node to another. The dimensioning results in the counting of used resources after having executed the routing phase. Different criteria for choosing a path can be considered; each of them enables the optimization of a particular parameter giving different optimal resource dimensioning.

This section is divided into three parts: first we explain the modifications to an existing routing tool when transparency is introduced; then we explain the survivability problem and the new perspectives linked to automatic reconfiguration; and finally the challenges related to the dynamicity and automation of working network are discussed.

3.1. Evolution of planning tool for transparent network

In an opaque network, dimensioning boils down to computing the route associated to each demand according to available free channels. Demand blocking occurs only if there are not enough resources (free wavelength and/or optoelectronic converter) [10].

In a transparent/hybrid network, the routing phase has to consider the constraints due to the lack of optoelectronic conversions:

1. *Wavelength continuity*: on each link of the lightpath, i.e. the taken wavelength has to be the same. The lightpath is the transparent section of a path between two OEO conversions. If the wavelength continuity is not guaranteed, a wavelength conversion is required.

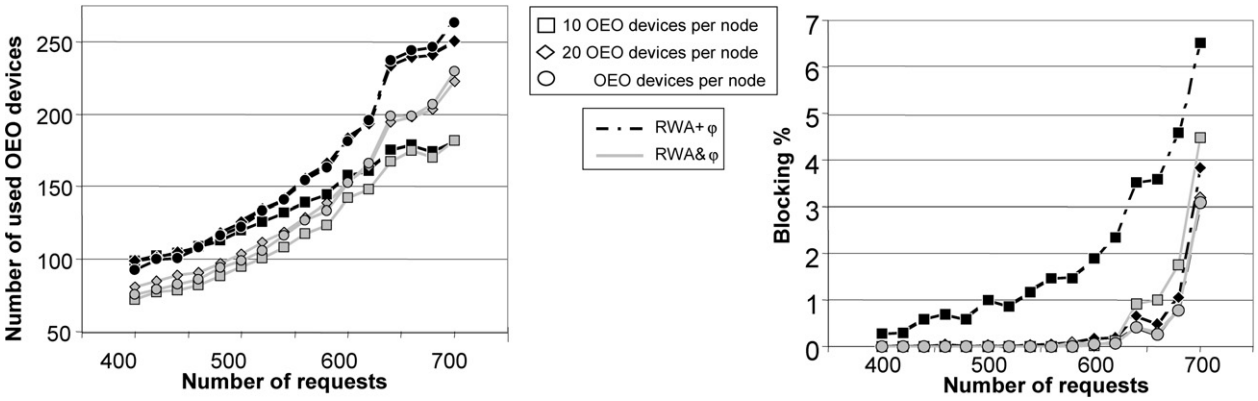

Fig. 6. Comparison of the reduction in the number of used OEO devices in the cases of RWA+φ and RWA&φ algorithms and the blocking demand due to the limitation of OEO devices.

2. *Physical feasibility*: the impairments due to propagation and switching accumulate along the link, the good reception of the lightpath on the receiver has to be guaranteed. If the signal is too degraded optoelectronic regeneration is performed.

The initial study considering the search for the route is divided into two parts: routing (choice of the suitable path) – R – and wavelength assignment (allocation of an available wavelength for such path) – WA. These sub-problems can be solved separately, first routing and then wavelength assignment (R+WA), or jointly (R&WA). Chen et al. [21] have shown that R&WA performs better than R+WA as it considers the wavelength availability during the path search process. In the following we will always refer to R&WA.

In order to integrate physical constraints, recent routing solutions include the role of the physical layer in setting up lightpaths by employing appropriate models such that the transmission quality (expressed by the Q-factor or the bit error rate – BER) of a candidate lightpath could be estimated in advance to determine its feasibility. Impairment constraints-based routing (ICBR) algorithms have been developed in [22].

It is possible to check the physical feasibility after the RWA phase, RWA+φ (using previous nomenclature), or during this phase, RWA&φ; φ denotes the physical constraint. Comparing RWA+φ and RWA&φ, best results are obtained with the second method because the selected path is, for construction, feasible and OEO devices are optimized to perform both wavelength conversion and signal regeneration. Fig. 6 shows the reduction in the number of OEO devices in the cases of RWA+φ and RWA&φ algorithms, for the network parameters used in Fig. 2. For this study we suppose to vary the number of total connections to route in the network (number of requests). The performance comparison of RWA+φ and RWA&φ routing is made counting the number of total OEO resources required to route demands. In terms of dimensioning, the best results are obtained when for the same number of request a method needs fewer OEO resources. Here we suppose that 10, 20 or an infinite number of OEO regenerators are available in each node. We observe that in the RWA&φ case the use of intermediate OEO regenerations is always reduced when we compare the used devices for the same number of routed demands, reaching a maximal reduction of 20% (curve relative to '∞ OEO devices per node'). Observing the curve relative to '10 OEO devices per node' RWA&φ routing we observe an initial divergence in the number of OEO devices from the one relative to the respective RWA+φ and, compared to the curves relative to other availability of devices per node that remain separated, the RWA&φ performs as RWA+φ. But if we observe the right-side of the figure, representing the blocking ratio (number of non-routed demands for lack of resources) we observe that it is fewer for RWA&φ, that means that the same required OEO resources to transport more demands, i.e. RWA&φ performs better.

3.2. Evolution of survivability strategies: protection versus restoration

A network carries an amount of data, proportional to the transported bit rate. The amount of lost data in case of a failure (in a time frame) increases with the bit rate and it is imperative to solve the survivability (complete transport

of a signal in case of failure) problem in advance. Most networks have to be able to quickly detect, isolate and recover from a failure; this issue is addressed in a huge number of studies [7].

Today, to ensure the fast recovery request, the survivability of a demand is made with dedicated $(1 + 1)$ protection because recovery is not conceivable if switching operations are not automatic and if devices are not tunable. In the dedicated protection each signal is transmitted on two different connections employing different resources (to avoid shared points of failure, that is the possibility to have common points that can fail and affect both connections); both these connections are active.

The main advantage of dedicated protection consists in the rapid activation of the backup path (faster than 50 ms, the required time for activation of protection in SONET specifications [18]). On the other hand, this solution is expensive because all required protection resources (time/space channels, wavelengths) are allocated before the failure and cannot be shared.

Restoration consists in searching and/or establishing a new path once a fault in the network has been detected.

If the search phase is computed before the failure, the occupation of backup resources is not done before the failure arises. In this case the backup resources can be shared by other traffic (having less important request on the quality of service) prior to the failure event. However, when a failure arises some constraints appear such as signaling (to reserve the necessary resources for the backup) propagation delay, cross-connect time to change configuration and check the new one; all these operations need time and make hard it to achieve the goal of 50 ms. Experimental results [19] and [20] show that this protection option is able to restore traffic within several hundred milliseconds. Dynamic restoration is called the solution with both search and establishment of the restoration path; it has become possible thanks to the introduction of dynamic and automatic devices. This option is the most cost efficient and least capacity consuming because the found restoration path is adapted to the network traffic state when the failure occurs, but needs a longer restoration time. As in the previous case, dynamic restoration needs signalization time but also path computation time. The path computation time depends on the choice of network management [7]. Another advantage of dynamic restoration is its greater resilience to traffic evolution because there is the sharing resource opportunity.

Different restoration strategies exist as a function of the re-establishment time or optimization of global resources [7].

3.3. Dynamic networks

In a dynamic scenario, optical connections are set up or released at any time to scale the traffic. This adds new constraints to the routing algorithm conception such as:

- Non-predictability of future connection requests;
- Very fast path computation;
- Information gathering.

3.3.1. Non-predictability

In a static network the traffic matrix is known in advance and a full routing optimization can be performed offline. On the contrary, in a dynamic network, the operator does not know in advance how many and which connections will be set up and/or released. When a new connection request is generated, the routing process deals with already established connections and available resources (bandwidth, regeneration devices, switch size) that have been previously computed during the design phase considering a forecast of future traffic and its behavior. Usually dynamic routing results are sub-optimal: there is an extra use of resources compared to the case in which all requests are known in advance (static case); the random installation and release of connections induce the fragmentation of fiber capacity [23]. Different routing strategies using heuristics are implemented to limit the sub-optimality problem (load balancing, wavelength assignment strategies…) [24]. Currently, the best solution is the re-arrangement of already routed demands, as shown in [23–25].

3.3.2. Fast computation

In dynamic networks, when a demand is received, the set-up process has to be as fast as possible. Such a process is divided into routing the path associated to the demand, reserving all resources required by it and lighting up the signal. The two last processes need times that cannot be reduced for messaging and processing and require some ms [26].

Even if computational power doubles every year (following the Moore's law) and efficient shortest-path algorithms exist in the literature (e.g. A^*), the huge amount of processed information increases computation time [6]. Today many studies are being conducted to find a trade-off between efficiency and rapidity. The interest of these studies consists also in understanding which architecture (centralized or distributed as defined in the following section) has to be adopted for an automatic transparent network.

In automatic opaque optical network GMPLS has been introduced to enable automatic channel setup for incoming demands; many works and discussions have been in debate last years to adapt the routing and signaling protocols in GMPLS for transparent/hybrid networks [27].

3.3.3. Information gathering

Routing requires input parameters describing the network state at a time "t" (equipment state (on/down), wavelength occupation, regeneration location) [28]. There are two paradigms for the management of these parameters: "*centralized*" and "*distributed*". In the former, only one entity handles the routing processes; it has a complete framework of the network and performs the best possible routing but at the price of a complex computation and a heavy signalization system. In the latter, each node is able to perform the routing owing to its own database about the network state. However, to up-date these database each node must exchange information with the others via an appropriate protocol at regular intervals of time [29]; more bandwidth is consumed as the intervals become shorter. The network state can change at any time and if the update interval is too large, there is the risk of using a non-available route due to out of date information. The choice of paradigm is still under discussion.

4. Quality of transmission estimator

In Section 3 we asserted the efficiency of algorithms performing the physical estimation of a signal during the routing process. Different models are proposed in the literature to evaluate the performance of the propagated signals. In order to be included into a routing algorithm, physical impairment estimators must present both computational simplicity and an accurate estimation. These requirements are more restrictive if the estimator has to be integrated in the control plane to ensure the automatic calculation and physical connection of new requests [27]. To be integrated in a control plane, the estimator employed by a routing algorithm has to:

1. be expressed by a simple analytic formula and be easily integrable (computation load);
2. exhibit a good accuracy (precision of the estimation).

However, simplicity and accuracy are exclusive goals. Accurate impairment models are based on the solution of a non-linear Schrödinger equation, but such methods are time consuming and inappropriate for routing algorithms. In the following we present one Quality of Transmission (QoT) estimator developed for non-return to zero (NRZ) modulated signals at 10 Gbit/s on a single mode fiber (SMF), [30,31], that is a compromise between fast computation and accurate estimation. This method can be adapted to any modulation format and to any bit rate; the scope of the following paragraphs is to explain the method to establish the estimator. Other estimators can be found in the literature [32,33].

4.1. Quality of Transmission – QoT

The quality of transmission function associates a Q-factor (expressed in dB) relative to a BER [34] assuming a Gaussian distribution of the noise and using relation (1):

$$BER = \frac{1}{2} \cdot \operatorname{erfc}\left(\frac{Q_l}{\sqrt{2}}\right) \approx \frac{1}{\sqrt{2\pi}} \frac{\mathrm{e}^{-Q_l^2/2}}{Q_l} \quad \text{with } Q_l = 10^{Q/20} \tag{1}$$

Indeed, following the trend derived from the assumption of Gaussian distribution for the intensity noise after detection, the Q-factor (dB) happens to depend linearly, in a first approximation, on the OSNR (in dB) measured in a reference bandwidth such as 0.1 nm, for common OSNR values between 10–23 dB (0.1 nm^{-1}). The Q-factor is a function of the impairments that the signal experienced during the propagation: the amplified spontaneous emission (ASE) noise

(and thus indirectly the OSNR), the accumulated chromatic dispersion (D_{res}), the non-linear phase (φ_{nl}) as defined in [35], the PMD, and the cross-talk (Xtalk). The Q-factor can be written as:

$$Q = \zeta(D_{\text{res}}, \varphi_{\text{nl}})OSNR + g(D_{\text{res}}, \varphi_{\text{nl}}, PMD, Xtalk) \tag{2}$$

For the systems considered in this study the penalties due to filter distortions and out of band distortion at the node can be neglected, because [36] demonstrates that for 10 Gb/s channels with 50 GHz spacing and NRZ modulation format these effects do not induce considerable penalties.

The $g(\cdot)$ function accounts for the penalties accumulated along the transmission: chromatic dispersion, non-linear phase, PMD and Xtalk. The $\zeta(\cdot)$ function accounts for patterning effects occurring during transmission due to chromatic dispersion and non-linear effects. $\zeta(\cdot)$ is at most 1 (high OSNR case) but can decrease down to 0.5 in the case of high non-linear effects during transmission. To relate this model with measurements or numerical simulations, we measure (or calculate) the required OSNR at the end of a given lightpath, $OSNR_{\text{ref}}$, to determine a reference value of $Q = Q_{\text{ref}}$. Q_{ref} corresponds to the performance that we want to interpolate with the best accuracy and to the decision threshold concerning the feasibility of a transparent lightpath. ($Q_{\text{ref}} = 12.6$ dB for a BER of 10^{-5}). $OSNR_{\text{ref}}$ is a function of the parameters D_{res}, φ_{nl}, PMD, and $Xtalk$. Hence Eq. (2) can be modified as follows:

$$Q = Q_{\text{ref}} + \zeta(D_{\text{res}}, \varphi_{\text{nl}})\big(OSNR - OSNR_{\text{ref}}(D_{\text{res}}, \varphi_{\text{nl}}, PMD, Xtalk)\big) \tag{3}$$

Let $OSNR_{\text{BtB}}$ be the OSNR corresponding to Q_{ref} in the back-to-back configuration (measured with a transmitter and receiver connected together without any transmission line in between) and $Pen_{\text{Qref}}(D_{\text{res}}, \varphi_{\text{nl}}, PMD, Xtalk) = (OSNR_{\text{ref}}(D_{\text{res}}, \varphi_{\text{nl}}, PMD, Xtalk) - OSNR_{\text{BtB}})$ the OSNR penalty due to the transmission at $Q = Q_{\text{ref}}$; thus Eq. (3) becomes:

$$Q = Q_{\text{ref}} + \zeta(D_{\text{res}}, \varphi_{\text{nl}})\big(OSNR - OSNR_{\text{BtB}} - Pen_{\text{Qref}}(D_{\text{res}}, \varphi_{\text{nl}}, PMD, Xtalk)\big) \tag{4}$$

Signal degradations can be divided into two classes: the ones that distort signal pulses (CD, PMD, non-linear phase), and the ones that increase noise around marks, '1', and spaces, '0', (ASE, crosstalk). These two types of degradations can be considered independent from each other and justify the penalty separation of crosstalk and ASE from other effects, in a first approximation. Penalties of crosstalk and OSNR should be separated as the resulting power distributions are different [37]. Zyskind et al. [38] showed that penalties due to chromatic dispersion are related to non-linear phase values. Furthermore in a first order approximation, these penalties are independent of PMD values [39]. With these assumptions, we rewrite Eq. (4) as follows:

$$Q = Q_{\text{ref}} + \zeta(D_{\text{res}}, \varphi_{\text{nl}})\big(OSNR - OSNR_{\text{BtB}} - Pen_{\text{Qref}}(D_{\text{res}}, \varphi_{\text{nl}}) - Pen_{\text{Qref}}(PMD) - Pen_{\text{Qref}}(Xtalk)\big) \tag{5}$$

Eq. (5) establishes that Q can be determined for any lightpath, thanks to the knowledge of the OSNR at the end of the transmission and the knowledge of the OSNR penalties for a given Q-factor (Q_{ref}).

Now, if we consider that Q_{ref} is also the threshold that allows making the decision whether or not the transmission on the lightpath is possible, we can write Eq. (5) as:

$$Q = Q_{\text{ref}} + m(D_{\text{res}}, \varphi_{\text{nl}}, PMD, Xtalk) \tag{6}$$

Here $m(D_{\text{res}}, \varphi_{\text{nl}}, PMD, Xtalk)$ expresses the Q-margin of the lightpath. If $m(D_{\text{res}}, \varphi_{\text{nl}}, PMD, Xtalk)$ is positive, the Q-factor is better than the reference Q-factor and the transmission on the considered line is possible. In the next section, we explain how we determine the different penalty terms.

4.2. Method for the interpolation of $Pen_{\text{Qref}}(D_{\text{res}}, \varphi_{\text{nl}})$

We focus our analysis on $Pen_{\text{Qref}}(D_{\text{res}}, \varphi_{\text{nl}})$, the penalty term due to chromatic dispersion and non-linearities appearing in Eq. (5). Experimental measurements or numerical simulations, described in the next paragraph, enable us to determine $Pen_{\text{Qref}}(D_{\text{res}}, \varphi_{\text{nl}})$ at a fixed reference BER (or Q_{ref}) as a function of the residual dispersion and the non-linear phase. The residual dispersion is the accumulated dispersion on transmission and compensation fibers; it is called residual because depends on the partial fulfilled compensation (it depends on considered wavelength, quality of DCF, measure accuracy, ...).

Fig. 7 gives an example of an OSNR penalty curve with respect to chromatic dispersion obtained for $\varphi_{\text{nl}} = 1.27$ rad (1800 km and a power of 3 dBm per channel).

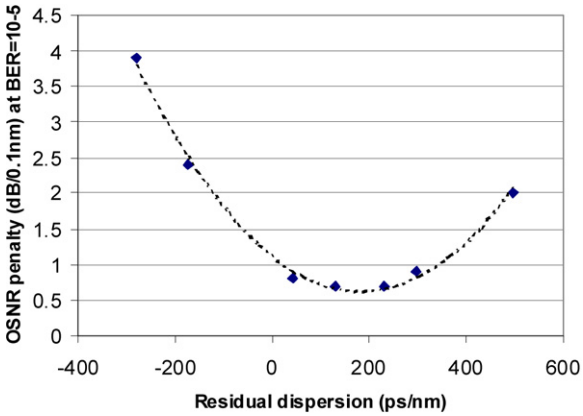

Fig. 7. Example of OSNR penalty versus the residual dispersion measured for $\varphi_{\mathrm{nl}} = 1.27$ rad. Diamonds are measured points and the dotted line is the interpolation.

We apply a two-step process to derive the relation: in the first step, we approximate each OSNR penalty versus the residual dispersion curve by a quadratic polynomial, as long as the penalty is less than 5 dB. Higher penalties are not considered because the precision of the estimation will be degraded, and for penalties greater than 5 dB no connections are possible.

$$Pen_{\mathrm{Qref}}(D_{\mathrm{res}}, \varphi_{\mathrm{NL}}) = a_{\varphi} D_{\mathrm{res}}^2 + b_{\varphi} D_{\mathrm{res}} + c_{\varphi} \tag{7}$$

In the second step, the coefficients a_{φ} , b_{φ} and c_{φ} are fitted by a polynomial of second (or fourth) degree as a function of φ_{nl}. The scope of the estimator is to have a good precision and not be too heavy in computation. Precision is obtained by the degree of the polynomial function; the complexity is reduced if such degree is lower. We look for the smallest degree that satisfies the best function precision. The OSNR penalty can be rewritten as:

$$Pen_{\mathrm{Qref}}(\varphi_{\mathrm{nl}}, D_{\mathrm{res}}) = \sum_{i=0}^{2} \left[\sum_{j=0}^{k} \alpha_{j,i} \varphi_{\mathrm{nl}}^{j} \right] D_{\mathrm{res}}^{i} \tag{8}$$

with $2 \leqslant k \leqslant 4$.

4.3. Experimental set-up

We have applied our method for the establishment of a QoT estimator using an experimental set up. This experimental set-up is based on a 10.7 Gbit/s SMF-based WDM transmission system that is emulated by a recirculating loop (see Fig. 8). It is made of three 100 km long spans of SMF fibre. An in-line Dispersion Compensation Fibre (DCF_1 in Fig. 8) spool under-compensates each span, in order to maintain a target residual dispersion per span of $+100$ ps/nm at 1550 nm (i.e. the cumulated dispersion of the line fibre span plus the following in-line DCF). After a loop section, comprising 3-spans sections, a DCF spool (DCF_2 on Fig. 8) resets the total dispersion to 0 ps/nm. The value of the pre-compensation (i.e. cumulated dispersion of the DCF at the link input, described as Pre-comp. in Fig. 8) is -860 ps/nm at 1550 nm. Eventually, dispersion D_{res} is varied at the receiver side using a tuneable post-chromatic dispersion compensator (Post-comp. in Fig. 8).

We propagate 21 channels spaced by 50 GHz for the central wavelength channel (1550.12 nm). The channel modulation format is No Return to Zero (NRZ) with a pseudo-random binary sequence (PRBS) of $2^{23} - 1$ bits at 10.7 Gbit/s. The nominal power per channel is measured at the input of each line fiber span and varies from 1 to 4 dBm. The power per channel at the input of the DCF modules is 7 dB lower than at the input of the SMF. The total transmission distance varies from 300 to 2400 km (1 to 8 loop laps). The PMD measured over a loop lap is 1.45 ps. A polarization scrambler has been introduced into the loop in order to reduce the loop polarization effects so as to only consider the penalties induced by the chromatic dispersion and the non-linear phase. PMD induced penalties will be considered independently.

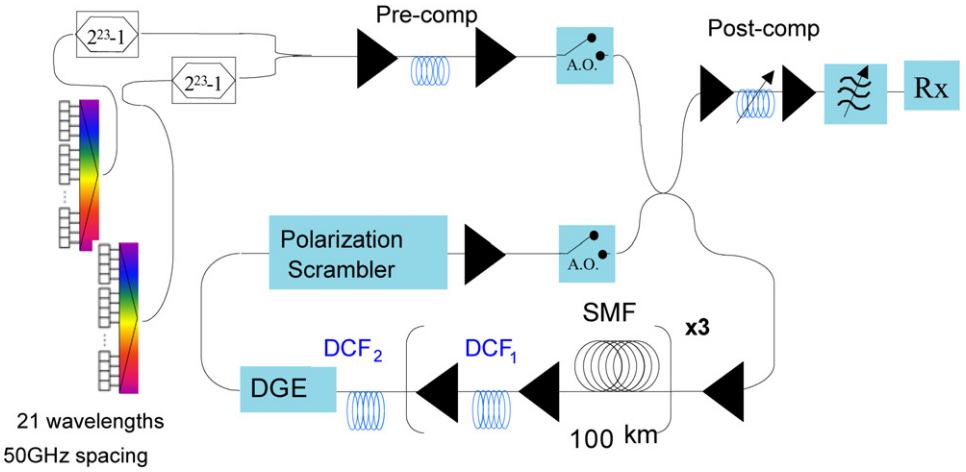

Fig. 8. Experimental set-up of the loop.

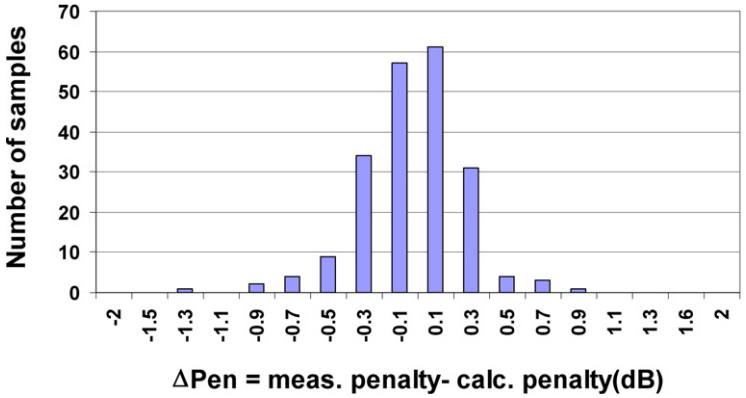

Fig. 9. Number of lightpaths versus the penalty differences ($Pen(measured) - Pen(estimated)$) for the experimental set up.

Fig. 9 shows the precision of the estimator. For all the 230 measured lightpaths, obtained by varying the number of loop lap and the post-compensation , we have calculated the difference between the measured OSNR penalty (Pen_{Qref} of Eq. (7)) and the OSNR penalty calculated by means of our estimator for the same values of chromatic dispersion and non-linear phase. By fitting this distribution with a Gaussian curve, we find that the estimation is within ± 0.5 dB for 91.5% of samples, ± 1 dB for 98.6% and ± 2 dB for 99.97 of the samples.

This estimator is a worst case for the transmission performance of lightpaths that are considered in a real network as it considers a perfect in-line residual chromatic dispersion reset to zero. In addition, the problem of this approach is that the measured samples are not representative of all possible configurations of chromatic dispersion and non-linear phase, number of spans per link, measure uncertainties .... It is not very easy to obtain it by an experimental set-up. For this reason in the following section we present an estimator, constructed by the same analysis but obtained using numerical simulations.

4.4. Simulations

A refined estimator, assuming a more realistic dispersion map, has been established using numerical simulations in [31]. Many configurations taking into account the uncertainties on the dispersion map and various distances between nodes have been simulated.

We simulate a transmission with a channel bit rate of 10.7 Gb/s and a NRZ modulation format. The sequence length is 64 bits and the extinction ratio is 13 dB. The dispersion map is identical to the one described above for the experimental circulating loop, except that, instead of varying the post-compensation fiber, it is set such as to compen-

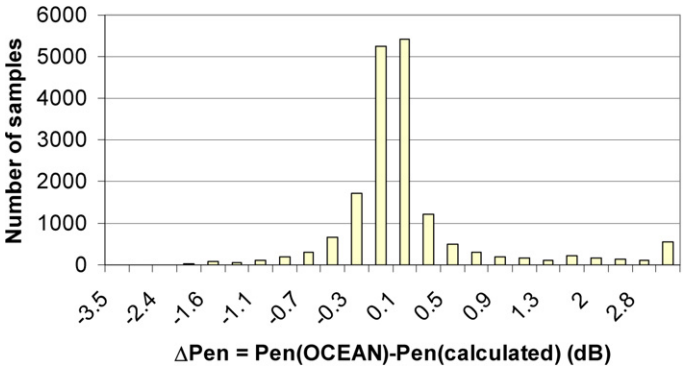

Fig. 10. Number of lightpaths versus the penalty differences ($Pen(simu) - Pen(estimated)$) for all considered non-linear phases.

sate for the pre-compensating fiber. We assumed a realistic chromatic dispersion map that presented uncertainties. For a given product of distance and power per channel (e.g. a specific non-linear phase), 800 simulations were performed: each simulation was done with a specific dispersion map which uncertainties had a Gaussian distribution with a standard deviation of $\sigma_1 = 5$ km for the SMF span length, $\sigma_2 = 0.2$ ps/nm/km for the SMF in-line chromatic dispersion and $\sigma_3 = 0.15$ ps/nm/km for the DCF in-line chromatic dispersion. Simulations are also performed with specific time delays between WDM channels that were chosen randomly between 0 ps and 6400 ps at the ingress node.

The input power per channel in SMF spans is set to 0 dBm and 3 dBm. Non-linear phases up to 2 rad are reached. Amplifiers have a flat gain over the C-band. Noise is generated at the receiver side. Because of the important chromatic dispersion of the SMF, the four wave mixing (FWM) impact is weak compared to the self-phase modulation (SPM) and cross-phase modulation (XPM). This is the reason why FWM is neglected in our simulations.

We emulated lightpaths and calculated the OSNR penalty obtained at a reference Q-factor *Qref*. The QoT function could be derived, expressing the Q-factor as a function of the cumulated residual chromatic dispersion and the non-linear phase.

In Fig. 10, we illustrate the number of lightpaths as a function of the difference between the calculated Q-factor using our simulation tool and the estimated Q-factor. The estimation is within ± 0.5 dB for 84.4% of the lightpaths.

We have calculated the performance of lightpaths having connection feasibility more likely to be critical, i.e. lightpaths with a length comprised between 2000 km and 4000 km. We considered a number of spans per link ranging from 3 to 6. It is important to note that due to a more regular reset at the nodes of the in-line residual chromatic dispersion, the 3-spans based QoT estimator corresponds to a worst case for the transmission performance when it is applied to lightpaths with 4, 5 or 6 spans per link.

We can calculate the Q-factor of each lightpath using our simulation tool and the Q-factor estimated by the derived QoT. If we assume that the numerical simulation represents the reference value of the Q-factor of a lightpath, we can compare the number of prediction errors, made using the estimator. For this we compare the prediction of the connection feasibility for each lightpath using the numerically calculated Q-factor and the Q-factor calculated with the QoT estimator. We find that the error on the prediction made by the estimator for all simulated lightpaths is 5.4%.

4.5. Simulated versus experimental results

We are able to correlate the experimental and simulated results. We simulated the circulating loop with the chromatic dispersion map described previously. The calculation was done for random temporal delays between channels taken between 0 ps and 6400 ps corresponding to one sequence length. For each non-linear phase, the calculated BER with the different temporal delays has been averaged. Fig. 11 depicts the comparison of the OSNR penalty obtained by experimental measurements (triangles) and simulations (squares) with respect to the non-linear phase for 0 ps/nm of total residual dispersion at 1550.12 nm. For a lightpath with a non-linear phase larger than 1.5 rad, the calculation tends to be pessimistic compared to the experimental results, making the estimator more conservative with respect to the measured lightpaths.

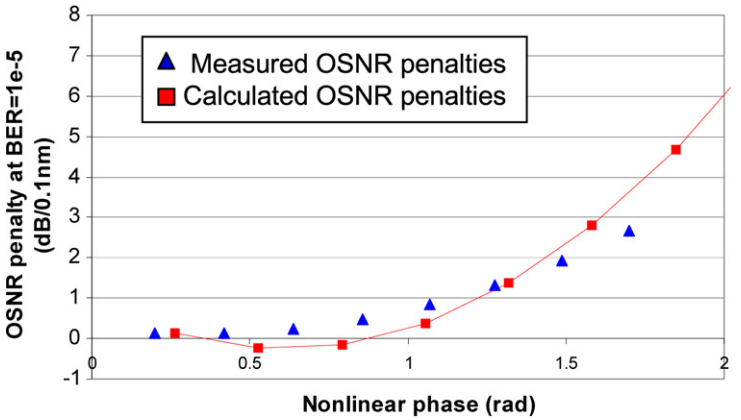

Fig. 11. Measured (triangles) and simulated (squares) OSNR penalty as a function of the non-linear phase for a cumulated dispersion of 0 ps/nm at 1550.12 nm.

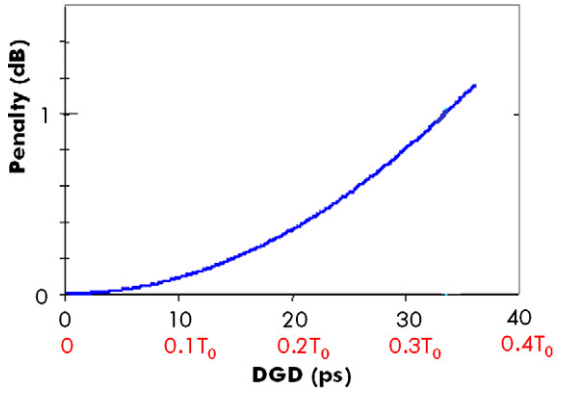

Fig. 12. Measured OSNR penalty versus DGD for 10 Gb/s NRZ signal.

4.6. *Method for the interpolation of Pen_{Qref} (PMD) and Pen_{Qref} (Xtalk)*

The penalty dependence on PMD, PenQref(PMD), can be derived from measurements of the penalty function with respect to DGD (Differential Group Delay). On Fig. 12, we have represented the measured OSNR penalty as a function of the DGD for a 10 Gb/s NRZ signal. On this figure, T_0 represents the bit duration. Such a measurement allows deriving the induced penalty, knowing the DGD of the birefringent material that supports the transmission.

Assuming the Maxwellian nature of the statistics of the DGD probability density function of the fibres, parameterized by its mean value (the PMD), we can derive from a PMD value, the maximum DGD, DGD_{th}, corresponding to an outage probability of 10^{-5} (i.e. 99.999% of the links have a probability to have a DGD lower than DGD_{th}, [40]). Thus we can easily derive the maximum expectable OSNR penalty with such an outage probability: it just consists in a change of scales in the relationship between penalty and DGD (Fig. 12, [40]) to get the relationship between the expectable penalty and the PMD. In the following, we approximate this PenQref(PMD) function by a second order polynomial function, based on standard penalty versus DGD curves for NRZ format.

4.7. *Network dimensioning*

Fig. 13(a) represents the repartition of the ligthpaths for an American network as a function of the distance for two models of traffic, uniform and T1. The American network is composed of 46 nodes and 61 links, the average link length is 400 km. [6] contains more information about the network. The uniform traffic is obtained considering the same probability for demands between two nodes in the network; T1 is created increasing the probability for shortest connections. Calculations of the number of required regenerators in Fig. 12(b) were made using the dimensioning tool

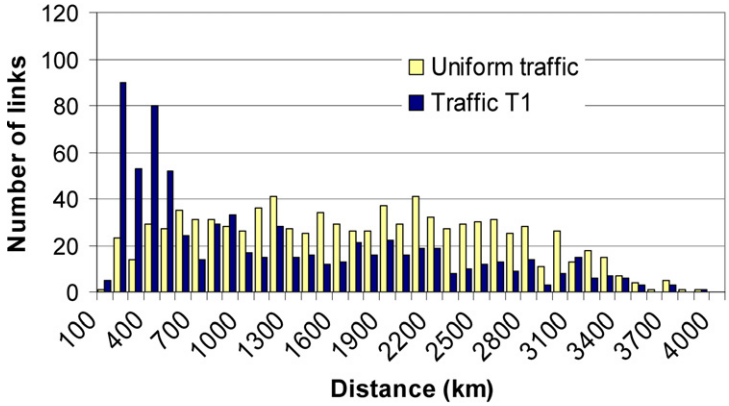

(a)

	T-Unif	T1
QoT	159	20
D-Max	289	83

(b)

Fig. 13. (a) US core network. The number of links is represented as a function of the distance for a uniform traffic and traffic T_1. (b) Number of required regenerators using the QoT estimator and the Max-D criterion.

described in Section 3 with two different estimators: the first estimator is the one described in Section 4 and the second is the Maximum Distance (Max-D) criterion. The Max-D is the maximum propagation distance without regeneration for which all wavelengths satisfy Eq. (2). The network parameters (flat gain amplifiers, fiber characteristics, PMD and crosstalk) are the same as the ones in the previous simulations. We can see in Fig. 13b, that the uniform traffic in overall requires more regenerators (longer connections). From such figure we observe that the use of the QoT estimator saves many regenerators (45% and 65% saving respectively for Uniform and T1 traffic) compared to the Max-D criterion because it predicts more precisely the performance than the Max-D which under-estimates the performance of many links and leads to an over-dimensioning of the network. More details are given in [31].

5. Conclusions

Optical transparency allows the evolution toward next generation networks that will provide rapid service provisioning, capacity upgrade with no interruption of current traffic, cost effectiveness and survivability. To achieve such goals, new technological challenges are involved in the switching, in the intelligent management of the network and in the planning tools for the dimensioning of the network. In this article, we have summarized the advances in optical switching technologies that enable the flexibility of the network and we also have discussed the tools, such as monitoring, that give "intelligence" to the network. Regarding the dimensioning of the network, the routing process has to be optimized for an efficient and economic management of the resources. Moreover, the integration of physical parameters in the planning tools allows an optimized management of the resources involved in the static dimensioning but also to face the requirements for dynamic allocation as well as protection and restoration.

Acknowledgement

The authors would like to thank Dominique Verchère for fruitful discussions.

References

[1] X. Yang, B. Ramamurthy, Dynamic routing in translucent WDM optical networks: The intradomain case, Journal of Lightwave Technology 23 (3) (March 2005) 955–971.
[2] G. 8080, Architecture for the automatically switched optical network (ASON), 2006 Revision – to be published imminently.

[3] D. Papadimitriou, D. Verchere, GMPLS user-network interface in support of end-to-end rerouting, IEEE Communication Magazine 43 (7) (July 2005) 35–43.
[4] D.C. Kilper, et al., Optical performance monitoring, Journal of Lightwave Technology 22 (1) (January 2004) 294–304.
[5] J.C. Antona et al., Performance & physical design of heterogeneous optical transmission systems, Comptes Rendus Physique 2008, submitted for publication.
[6] A. Morea, et al., QoT function and A^* routing: an optimized combination for connection search in translucent networks, OSA Journal of Optical Networking 7 (1) (January 2008).
[7] G. Ellinas, et al., Network control and management challenges in opaque networks utilizing transparent optical switches, IEEE Communication Magazine (February 2004).
[8] ITU-T Reccomendation G.652, 2005.
[9] ITU-T Reccomendation, G.655, 2006.
[10] E. Bouillet, et al., Path Routing in Mesh Optical Networks, Wiley Editorial Offices, 2007.
[11] A. Morea, I. Boyer-Hear, Availability of translucent networks based on wss nodes, comparison with opaque networks, in: Proceedings IEEE Networks 2006.
[12] A. Morea, J. Poirrier, A critical analysis of the possible cost savings of translucent networks, in: Proceedings IEEE DRCN05, 2005.
[13] T. Ducellier, et al., Novel high performance hybrid waveguide – MEMs 1×9 wavelength selective switch in a 32-cascade loop experiment, in: Proceedings IEEE ECOC04, 2004.
[14] K. Tse, AT&T's photonic network, in: Proceedings IEEE/OSA OFC08, 2008.
[15] H. Bulow, et al., Outage dynamics of 40 Gb/s optical paths routed over PMD-impaired fiber links, in: Proceedings OSA/IEEE OFC08, 2008.
[16] I. Tomkos, et al., Dynamic impairment constraint optical networking: the activities of DICONET EU project, in: OFC 2008 Workshop on Network Planning Tools.
[17] T. Zami, et al., Driving technologies addressing the future dynamic transparent core networks, in: Proceedings of IEEE ICTON08, 2008.
[18] G. Suwala, G. Swallow, SONET/SDH – like resilience for IP networks: a survey of traffic protection mechanisms, in: IEEE Network, March/Avril 2004.
[19] G. Li, et al., Experiment in fast restoration using GMPLS in optical/electronic mesh networks, in: Proceedings of OFC01, 2001.
[20] R.D. Doverspike, et al., Fast restoration in a mesh network of optical cross-connect, in: Proceedings of OFC99, 1999.
[21] C. Chen, S. Banerjee, A new model for optimal routing and wavelength assignment in wavelength division multiplexed optical networks, in: Proceedings IEEE Infocom96, 1996.
[22] I. Tomkos, et al., Impairment constraint based routing in mesh optical networks, in: Proceedings IEEE/OSA OFC07, 2007.
[23] T. Cinkler, et al., λ-path fragmentation and de-fragmentation through dynamic grooming, in: Proceedings IEEE ICTON 2005.
[24] I-Shyan Hwang, Shyh-Jye Luo, Load balance RWA algorithm using statistical analysis in WDM mesh networks, International Journal of Contemporary Mathematical Sciences 1 (10) (2006) 501–507.
[25] A.K. Kodi, A. Louri, A new dynamic bandwidth re-allocation technique in optically interconnected high-performance computing systems, in: Proceedings IEEE Symposium on High-Performance Interconnects 2006.
[26] B.T. Doshi, et al., Optical network design and restoration, Bell Labs Technical Journal (January–March 1999).
[27] R. Martinez, et al., Challenges and requirements for introducting impairment-awareness into the management and control plane ASON/GMPLS WDM networks, IEEE Communication Magazine 44 (December 2006) 76–86.
[28] J. Zhou, X. Yuan, A study of dynamic routing and wavelength assignment with imprecise network state information, in: Proceedings IEEE ICPPW02, 2002.
[29] A. Giorgetti, et al., Impact of link state advertisement in GMPLS-based wavelength-routed networks, in: Proceedings IEEE/OSA OFC08, 2008.
[30] B. Lavigne, et al., Method for the determination of a Quality-of-Transmission estimator along the lightpaths of partially transparent networks, in: Proceedings IEEE ECOC07, 2007.
[31] F. Leplingard, et al., Determination of the impact of a quality of transmission estimator margin on the dimensioning of an optical network, in: Proceedings IEEE/OSA OFC08, 2008.
[32] S. Pachnicke, Physical impairment based regenerator placement and routing in translucent optical networks, in: OSA IEEE OFC08, February 2008, paper OWA2.
[33] N. Madamopoulos, et al., Performance evaluation of a transparent reconfigurable metropolitan network under static and dynamic traffic, IEEE/OSA Journal of Lightwave Technology (2002).
[34] D. Marcuse, Derivation of analytical expressions for the bit-error probability in lightwave systems with optical amplifiers, Journal of Lightwave Technology 8 (12) (December 1990) 1816–1823.
[35] J.C. Antona, et al., Nonlinear cumulated phase as a criterion to assess performance of terrestrial WDM systems, in: Proceedings IEEE/OSA OFC02, 2002.
[36] J.D. Downie, A.B. Ruffin, Analysis of signal distortion and crosstalk penalties induced by optical filters in optical networks, IEEE Journal of Lightwave Technologies 21 (2003) 1876–1886.
[37] T. Zami, et al., Crosstalk-induced degradation in an optical-noise-limited detection system, in: Proc. of IEEE/OSA OFC1999, February 1999, pp. 255–257.
[38] J. Zyskind, et al., High-capacity, ultra-long-haul networks, in: I. Kaminov, T. Li (Eds.), Optical Fiber Telecommunication IVB, Systems and Impairments, Academic Press, Elsevier Science Imprint, 2002, pp. 198–231.
[39] H. Kogelnik, et al., Polarization-mode dispersion, in: I. Kaminov, T. Li (Eds.), Optical Fiber Telecommunication IVB, Systems and Impairments, Academic Press, Elsevier Science Imprint, 2002, pp. 725–861.
[40] ITU-T, Recommandation G.691, Optical interfaces for single channel STM-64, STM-256 and other SDH systems with optical interfaces, ITU 2000.